Limit Cycle Mixing

L. MAHRT*

Department of Atmospheric Sciences, Oregon State University, Corvallis, Oregon

(Manuscript received 5 February 1988, in final form 15 August 1988)

ABSTRACT

Lagrangian equations for momentum and buoyancy are developed for idealized turbulent fluid elements. The resulting formulation of transport can be viewed as a generalization of mixing length and parcel theories of mixing for application to gridded Eulerian models. This formulation of transport recognizes the mean gradients on the scale of the main transporting eddies and avoids problems with existing methods due to parameterization of fluxes in terms of local gradients between adjacent grid levels.

The modeled fluid elements develop relative horizontal motions due to mean vertical shear. Shear-produced horizontal kinetic energy is converted to vertical kinetic energy through modeled pressure adjustments. The fluid element is decelerated through nonlinear pressure drag and small scale diffusion with the ambient fluid while vertical motions are constrained by stable stratification.

The linearized version of the equations reproduces classical shear instability governed by a critical Richardson number. With nonlinear pressure drag and small scale diffusion, the element motion adjusts to limit cycle conditions which transport heat and momentum. The limit cycle motion varies from a buoyancy oscillation for large Richardson number to a bimodal limit cycle for small Richardson number. Due to momentum transport by pressure fluctuations, the eddy Prandtl number for stable stratification is generally greater than 1 and increases with stability.

1. Introduction

Atmospheric mixing by turbulence and convection is normally formulated in terms of a local flux-gradient relationship typically involving eddy diffusivity or mixing length formulations. With higher moment theory, the application of the eddy diffusivity closure occurs in the budget equations for the covariances rather than directly in the flux-relationship. Most models of turbulent transport are posed in terms of gridded numerical models.

Stull (1984), Wyngaard and Brost (1984), Wyngaard (1984), Fiedler (1984) and others have generically criticized such models in that the eddy flux is related to the local gradient between adjacent grid levels, whereas the actual eddies transport according to gradients on their own scale. In the heated boundary layer, it is necessary to apply corrections to the heat flux parameterized in terms of temperature gradients between adjacent grid levels, since, in reality, the thermals transport according to the bulk gradient across the entire boundary layer (Deardorff 1966). Failure to correct the local grid parameterization of the flux can even lead to the wrong sign in the relationship between the local flux and the local gradient. Deardorff's correction specifies an empirical parameter while the approach of Wyngaard and Brost (1984) is based upon the distinction between local flux due to upward transport from near the surface and local flux due to downward transport associated with entrainment at the boundary-layer top. The transilient approach (Stull 1984) specifies a matrix of mixing coefficients representing transport between all the different combinations of grid levels.

The present study pursues the problem of nonlocal mixing by constructing Lagrangian equations for idealized turbulent motions in order to estimate turbulent fluxes and other turbulence quantities. Previous Lagrangian or parcel models of turbulent or convective motions include Priestley and Ball (1955), Priestley (1959), Mason and Emig (1961), Lin and Reid (1963), Csanady (1964), Simpson and Wiggert (1969), Telford (1970), Krasnoff and Peskin (1971) and Pearson et al. (1983). A recent example of a Lagrangian or parcel approach for estimating mixing in Eulerian gridded models is the formulation of transport by thermals between the surface and other layers in the boundary-layer model applied in Zhang and Anthes (1982). As in the transilient method, the Lagrangian approaches can provide an estimate of the variation of the flux on the scale of the transporting eddies. The profile of this flux can then be transposed to the grid levels of a numerical model.

The present approach deviates from previous Lagrangian approaches in that it explicitly models the generation of vertical motions by pressure fluctuations induced by shear-generated horizontal velocity fluctuations. The turbulent length scale and eddy diffusivity

* Part of this work was carried out as a visitor to the Geophysics Institute, University of Bergen and the Bergen Scientific Centre.

Corresponding author address: Dr. Larry J. Mahrt, Atmospheric Sciences, Oregon State University, Corvallis, OR 97331-2209.

need not be specified with the present approach, but can be computed a posteriori as a product of the model. Previous models of mixing generally specify a mixing length or an eddy diffusivity either directly in the flux relationship, or, indirectly to close higher moment equations. Commonly used turbulence length scales include the depth of the boundary layer, distance from the ground, and w/N where w is a vertical velocity scale for the turbulence and N is the buoyancy frequency. This length scale is the vertical distance a parcel with initial vertical velocity w could travel before losing its kinetic energy to potential energy in the absence of pressure effects and mixing with the environment. After this vertical excursion, mixing length theory would then assume that the parcel completely mixes with the environment. However, this parcel argument is used only to justify the mixing length hypothesis which is then used to compute the eddy diffusivity. The flux is computed with this eddy diffusivity and the gradient between adjacent grid levels, not the gradient on the scale of the mixing length.

In these terms, *the present approach can be viewed as a generalization of the mixing length to include more complete Lagrangian physics and to relate the flux to the gradients on the scale of the transporting eddies.* With the present development, explicit specification of a vertical length scale or eddy diffusivity are replaced by the task of formulating the Lagrangian equations and interaction between the Lagrangian fluid element and mean vertical profiles as interpolated from the grid of the larger scale model. The formulation of the Lagrangian equations are not trivial because present parcel approaches do not accomodate the generation of eddy vertical motions from shear instability, a major task of the present approach. This process involves conversion of horizontal kinetic energy to vertical kinetic energy through pressure fluctuations, a process which is not completely understood.

The present development may be most useful in the stratified free atmosphere where present simple approaches are thwarted by the inability to estimate the turbulence length scale. In free turbulence, organization is no longer provided by a material surface such as the earth's surface. The behavior of the turbulent length scale is also poorly understood in strongly stratified boundary layers where relationship to the surface is uncertain and the transporting eddies may be intermittent and confined to thin layers. Therefore, this study will concentrate on the case of stably stratified, shear-generated turbulence in the absence of a material boundary although application to other cases will be of future interest.

The system of equations will be restricted to just a few degrees of freedom and therefore will still represent rather incomplete physics. This restriction allows explicit mathematical analysis of the model and elucidation of the various physical regimes. For example, we wish to establish the sensitivity of model results to initial conditions and parameter values. Furthermore, simplicity of the mixing model is absolutely necessary for formulation of fluxes within larger-scale models. Speziale (1987) has noticed that most modelers have shunned higher moment theory in favor of simple models of mixing for practical considerations.

Here, adequate mathematical simplicity will require omission of explicit representation of the internal structure and distortion of fluid elements. In many actual turbulent flows, it is not practical to observe fluid elements even approximately defined by material surfaces. Therefore the modeled Lagrangian elements can be viewed only as representation of the statistical influence of the turbulent eddies without consideration of the generation and decay of individual eddies. In other terms, the present development can be viewed as an extension of existing Lagrangian approaches to mixing and in fact includes some previous treatments as special cases (Section 2f).

The application of the modeled Lagrangian element to gridded models involves a number of decisions which depend on specific characteristics of the model. Such details are not included in this study which assumes a more general scope. In fact, the intention here is that the modeled Langrangian motion may also be suitable for a wider range of applications such as dispersion problems where the Lagrangian equations map a frequency distribution of fluid elements into a new frequency distribution at a later time.

2. Basic equations

We now formulate simplified equations for variables of fluid elements intended to represent the statistical behavior of transporting turbulent eddies. For simplicity we will consider only eddy motion in the plane of the shear, here the x–z plane. This assumes height-independent mean shear in which case there is no preferred direction for horizontal fluctuations perpendicular to the mean shear. For application to gridded models, it was necessary to add the second horizontal equation.

We begin with the basic equations for momentum and temperature for shallow motions without rotation (Dutton and Fichtl 1969; Mahrt 1986). We partition the flow into a basic state ambient flow $\Phi = (U, W, \Theta, P)$, deviations of fluid element variables from the basic state flow $\phi = (u, w, \theta, p)$ and smaller scale turbulence whose effect will be parameterized as a diffusive influence. We assume the basic state to be hydrostatic with negligible vertical motion ($W = 0$). The basic state horizontal flow U depends only on vertical height z. The derivative of the total flow can then be expanded as

$$d(\phi + \Phi)/dt = \partial\phi/\partial t + (u + U)\partial\phi/\partial x + w\partial\phi/\partial z + w\partial\Phi/\partial z = d\phi/dt + w\partial\Phi/\partial z$$

where the Lagrangian time derivative is defined as

$$d(\ )/dt = \partial(\ )/\partial t + (u + U)\partial(\ )/\partial x + w\partial(\ )/\partial z.$$

Noting the above simplifications for the basic state flow, we obtain the following equations for the deviation of the fluid element motion from the basic state flow:

$$dw/dt = g\theta/\Theta - (1/\rho_0)\partial p/\partial z - F_w \quad (1a)$$

$$du/dt = -wU_z - (1/\rho_0)\partial p/\partial x - F_u \quad (1b)$$

$$d\theta/dt = -wS - F_\theta \quad (1c)$$

where θ is the potential temperature replaced by virtual potential temperature in a moist atmosphere, or density in an incompressible fluid, Θ is its constant-scale value, S the vertical gradient of Θ in the basic state ambient flow, p the pressure, U_z the mean vertical shear of the horizontal flow, F represents the flux divergence due to diffusion by turbulence which is smaller scale than the fluid element, and ρ_0 is a constant basic state density. The above Lagrangian equations for w and θ of individual fluid elements can be found in Csanady (1964) and elsewhere. The equation for horizontal momentum u (1b) contains an additional term wU_z due to the presence of mean vertical shear in the present flow problem. The mean flow (U_z and S) might be specified or supplied by a coupled large scale model in which case the present development would serve as a submodel of turbulent transport.

The above three Lagrangian equations contain four unknowns. Since there is no mass continuity equation, an additional relationship for pressure is sought in subsections 2b and c below. The formulation for the small-scale diffusion terms is considered in the following subsection.

a. Small-scale turbulent diffusion

A Lagrangian fluid element will be modified due to the diffusive action of smaller-scale turbulence. That is, the total turbulent motion is superficially partitioned into the main coherent eddies responsible for most of the transport (modeled fluid elements) and the smaller scale turbulence which leads to diffusive exchange between the fluid element and its environment. In particular, we formulate the exchange of property ϕ between the fluid element and its environment according to the format

$$u_e\phi$$

where u_e is a velocity scale representing the small scale diffusion between the fluid element and ambient fluid, and $\phi = (u, w, \theta)$ is again the deviation of the fluid element variables from the basic state flow. The variables (u, w, θ) could be assumed to be average values over the fluid element. On the other hand, if the spatial variations within the fluid element are concentrated at the boundaries as a "jump" in properties, then u_e becomes an entrainment velocity.

The small-scale flux divergence appearing in (1) is then

$$F_\phi = u_e\phi/L \quad (2a)$$

where L is the length scale assumed to represent the smallest dimension of the fluid element which is in the expected direction of the maximum flux divergence. For example, in the heated boundary layer, L might be the average half width of the thermals. Note that the size of the fluid element $2L$ is probably much smaller than the vertical depth of the motion of the element determined by solution of the basic equations (1). For mechanically driven motions, the length scale L becomes less familiar compared to the case of thermals. In subsequent sections, we will study the role of the diffusion time scale L/u_e without concern for the numerical value or meaning of L.

The small-scale diffusion velocity u_e may approach one of two limits. In one limit, the small-scale turbulence is generated by the motion of the fluid element with an adjustment time scale which is small compared to the circulation time scale of the fluid element. Then the small scale turbulence is in equilibrium with the motion of the fluid element and the diffusion velocity is linearly proportional to the relative velocity of the fluid element. For this limiting case, (2a) becomes

$$F_\phi = C_e V\phi/L$$

$$V = (u^2 + w^2)^{1/2} \quad (2b)$$

where C_e is a nondimensional coefficient. This asymptotic case is the usual self-similar case (Priestley and Ball 1955; Turner 1973; and others), and leads to an expression for the momentum flux which depends quadratically on the velocity of the fluid element.

In the other asymptotic limit, the velocity scale for small-scale diffusion u_e appearing in (2a) is approximately constant during one circulation time scale of the fluid element. This limit might be a reasonable approximation if the small-scale turbulence is mainly associated with the ambient fluid or the time scale for the adjustment of the small-scale turbulence is long compared to the circulation time scale of the fluid element. In this case, the small-scale diffusion velocity is probably related to the overall velocity scale of the main eddies rather than their instantaneous velocity at a given level. With constant diffusion velocity u_e and element size L, the formulation for small-scale diffusion (2a) becomes linearly proportional to the deviation value of ϕ of the fluid element. The assumption of constant u_e/L is equivalent to specifying a constant diffusion time scale as invoked for momentum in the Lagrangian models of Csanady (1964) and for heat in Lin and Reid (1963) and Krasnoff and Peskin (1971) and others. The damping time scale in these models represent the effects of molecular diffusion, whereas the present approach requires formulation of diffusion by small scale turbulence. It is mathematically impor-

tant that the relationthip between the momentum diffusion and the relative speed of the fluid element is linear for this case.

Of course, the most appropriate formulation for the diffusion time scale L/u_e may vary between flow situations. In fact, Pearson et al. (1983) assume that the diffusion time scale for the momentum of fluid elements in stratified flow is proportional to the buoyancy time scale by arguing that the diffusion is accomplished primarily by internal gravity waves. They also assume that the diffusion time scale for heat is proportional to the buoyancy time scale.

If the time scale of the small scale turbulence is comparable to the circulation time scale of the fluid element, then asymptotic simplifications corresponding to constant diffusion time scale L/u_e or corresponding to self-similarity (2b) are not possible and a turbulence energy equation for the evolution of the small-scale turbulence is needed as in Telford (1970). This possibility becomes too complex for present requirements. We will proceed with relationship (2a) for the case of constant diffusion time scale.

b. Pressure drag

The influence of pressure gradient forces on the fluid element is quite complicated and involves the perturbation hydrostatic contribution as well as nonhydrostatic contributions due to pressure drag, shear-induced pressure fluctuations leading to conversion from horizontal momentum to vertical momentum and pressure perturbations induced by neighboring eddies. In some models, the pressure gradient force on the fluid element has been formulated in terms of a specified stationary random process (see Csanady 1964; Pearson et al. 1983 and references therein). In the present analysis, we will formulate the pressure drag and shear-pressure effect explicitly, but as simply as possible. This formulation will mark an important deviation of the present approach from the above approaches and from the Lagrangian theories noted in the Introduction and section 2f.

Pressure drag decelerates pulses of motion due to self-induced pressure gradient forces. More specifically, positive pressure perturbation (pressure head) develops at the leading edge of the motion (Fig. 1). This positive pressure perturbation is usually formulated as a quadratic function of the speed of the element as argued from scale analysis. As one example, such scaling arguments are used to justify the usual formulation of the pressure-work term in the turbulence energy equation (e.g., Tennekes and Lumley 1972, Eq. 3.2.33; Hinze 1975, sec. 3.8). The quadratic dependence of the pressure drag on relative flow speed is also argued by making an analogy between pulses of motion and the relative motion of solid objects in a fluid (Levine 1959 and others). Similar statistical results can be deduced from the divergence of the Navier–Stokes equation (Batchelor 1951). A quadratic relationship between the relative flow of a fluid element and the pressure force on the fluid element can also be derived by integrating the horizontal equation of motion for the internal structure of the element (List and Lozowski 1970, Eq. 6).

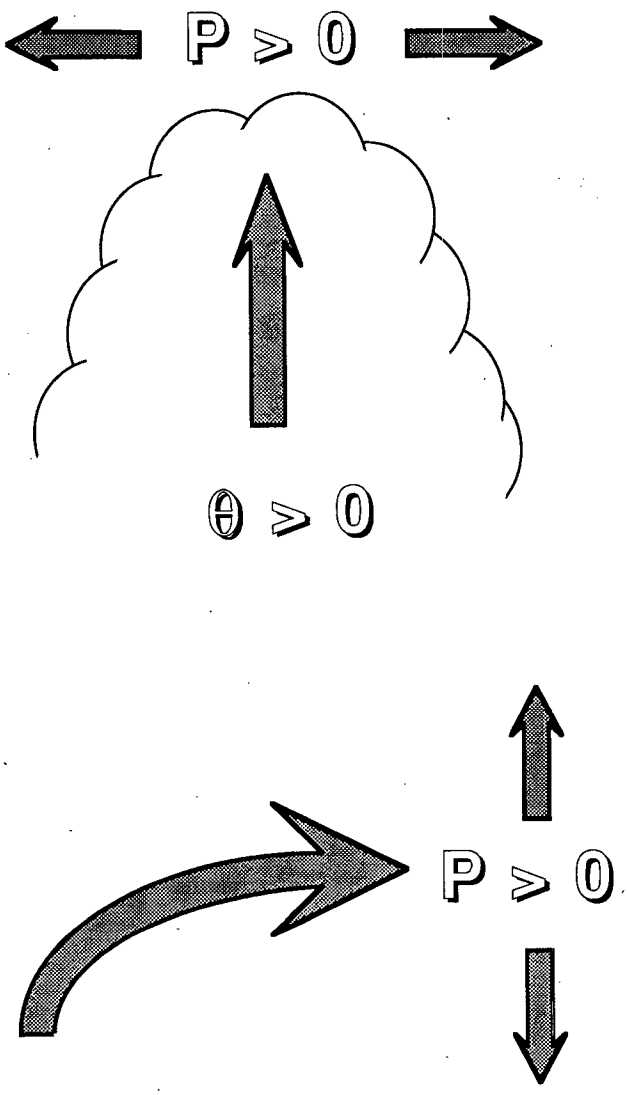

FIG. 1. Conversion of kinetic energy between velocity components due to pressure fluctuations induced by a vertical pulse of momentum (upper diagram), induced by a horizontal pulse of momentum (lower diagram).

With the above arguments, the pressure drag contributing to the pressure gradient terms in the vertical and horizontal equations of motion (1a–b) are of the form

$$C_p w V/L$$
$$C_p u V/L \qquad (3)$$

where C_p is a nondimensional coefficient thought to be O(1) (see references in Mahrt 1979) and assumed to be applicable to the pressure drag formulation for

both velocity components. In reality, C_p is probably quite variable and differs between flow components, especially in the presence of significant stratification. As the fluid element is distorted by the shear, the drag coefficient C_p may decrease. Although this effect will be referred to as pressure drag, this term can lead to absolute horizontal acceleration when the horizontal motion of the fluid element is slower than the ambient fluid. We will assume constant C_p/L.

Note that the pressure drag formulation (3) is the same mathematical form as the momentum diffusion term for self-similar turbulence where the diffusion velocity is proportional to the relative speed of the fluid element (2b). Therefore, self-similar diffusion could be included by augmenting the pressure drag coefficient C_p. Linear and quadratic "drag" forms arise in a wide variety of physical problems. In fact, some investigators have even proposed drag with a fractional exponent between the linear and quadratic forms (see, for example, Nayfeh and Mook 1979). As in previous situations, the linear and nonlinear drag effects in the present flow model will qualitatively exert quite different influences on the motion.

c. *Generation of vertical motions by pressure fluctuations*

The vertical shear of mean horizontal flow generates horizontal fluctuating motions in the direction of the mean shear. Such fluctuating motions induce pressure perturbations which, in turn, generate motions perpendicular to the mean shear (Fig. 1). Thus, the mean shear generates vertical motions indirectly through pressure fluctuations. In the Reynolds stress equation, this effect can occur through the so-called return-to-isotropy term involving correlations between fluctuations of pressure and velocity gradients.

An impression of how to formulate generation of vertical motion of the fluid element is provided by early conceptual views of shear instability. See, for example, Fig. 12 in Monin and Yaglom (1971) and Fig. 2a in this section. Perturbing the interface between two layers of fluid of different horizontal velocity leads to motion changes consistent with the Bernoulli relationship. The associated pressure changes act to further displace the interface and so on leading to instability.

The relative motion of any fluid element will generate pressure perturbations. If we consider the motion within the fluid element to be well mixed, the *relative* motion at the top of the fluid element will be different from that at the bottom of the fluid element due to the vertical variation of the mean horizontal flow (Figure 2b). We define the relative speed of the fluid element u with respect to the mean flow at the instantaneous mid-level of the fluid element, U_m. With this notation, the mean flow is $U_m + (\Delta z/2)U_z$ at the top of the fluid element of thickness Δz and $U_m - (\Delta z/2)U_z$ at the bottom of the fluid element. With the usual Bernoulli

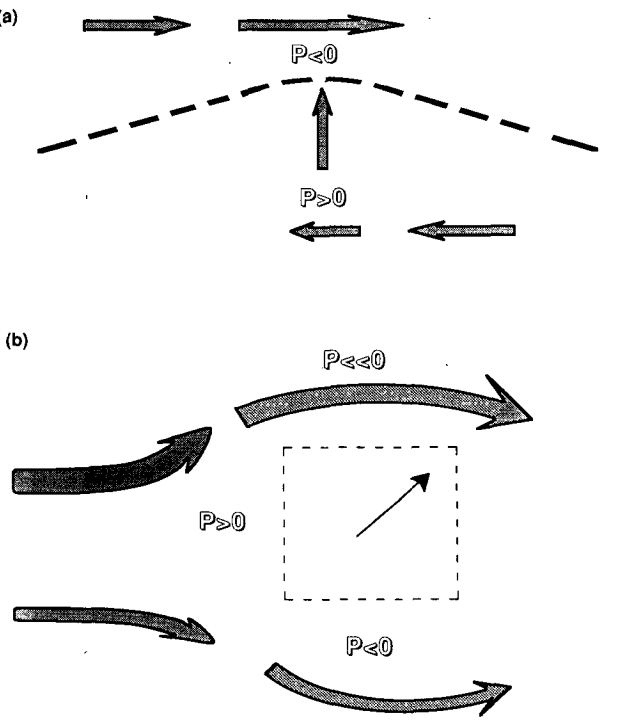

FIG. 2. Shear instability and associated pressure fluctuations for (a) an idealized interface and (b) an idealized fluid element.

argument, the perturbation pressure at the instantaneous top (z_T) of the homogeneous element is assumed to be quadratically proportional to the difference between the speed of the fluid element and the ambient flow speed at z_T and therefore of the form

$$p(z_T)/\rho \propto (-/+)(u - U_z\Delta z/2)^2. \qquad (4a)$$

The minus sign (pressure drop) is chosen if the ambient horizontal flow at z_T is faster than the speed of the fluid element and vice versa. For example, if the fluid element is rising in positive mean shear $U_z > 0$, then $u < 0$ leading to a relatively large pressure drop. At the instantaneous bottom (z_B) of the element, the perturbation pressure is

$$p(z_B)/\rho \propto (-/+)(u + U_z\Delta z/2)^2. \qquad (4b)$$

With these estimates U_z is the mean shear assumed to be constant in the neighborhood of the fluid element.

Using (4a–b), the vertical pressure gradient acting on the element is of the form

$$-(1/\rho_0)\partial p/\partial z = -CuU_z \qquad (5)$$

where the nondimensional coefficient C is proportional to the thickness of the element and proportional to a coefficient linking the perturbation pressure to the square of the relative velocity difference. This simple relationship recognizes that the perturbed pressure field is generated by the relative motion of the fluid element

u and that the vertical variation of the relative flow and perturbation pressure around the well-mixed fluid element is proportional to the mean shear.

The above Bernoulli arguments (4a–b) are not necessary in that formulation (5) can also be argued from dimensional analysis. In fact, the latter argument may be preferable in the stable case where it is hard to visualize a fluid element which is well mixed in momentum yet large enough to "see" the mean shear. Since relationship (5) represents a significant extension of the usual formulation of Lagrangian motions, it will require close scrutiny in subsequent sections.

d. Other pressure effects

The above treatments of the pressure field are still incomplete as can be seen by consulting Moeng and Wyngaard (1986). Here we note two additional effects which can be posed in a Lagrangian frame of reference. First, some have argued by analogy to the motion of solid objects that the element motion induces a pressure field which accelerates additional mass in the immediate environment of the element. This effect is formulated in terms of a virtual mass coefficient γ^* for the net acceleration (see references in Mahrt 1979). In this case, the sum of the virtual mass-pressure effect and the net acceleration becomes

$$dw/dt + \text{virtual mass effect} = \gamma^* dw/dt$$

$$du/dt + \text{virtual mass effect} = \gamma^* du/dt$$

where the nondimensional coefficient is somewhat greater than unity.

Second, the present formulation of the vertical equation of motion also fails to explicitly consider the hydrostatic contribution associated with the buoyancy field of the fluid element (Moeng and Wyngaard 1986) which might be included by specifying a coefficient which reduces the buoyancy term in the vertical equation of motion so that

$$-(1/\rho_0)\partial p_b/\partial z = -A(g/\Theta)\theta$$

where A is some fraction probably less than ½ (M. Hadfield, personal communication) and p_b is the part of the pressure associated with the buoyancy field. This pressure effect could involve initiation of internal gravity waves which propagate energy out of the neighborhood of the fluid element. The buoyancy-reduction pressure effect and the above virtual mass-pressure effect are not independent. The inclusion of these two effects in the present development is somewhat academic since each of the remaining terms in the vertical equation of motion contain coefficients with uncertain behavior.

We will therefore neglect these two pressure effects, in which case the pressure terms in the equations of motion reduce to the drag effect (3) and generation of vertical momentum from shear-induced pressure fluctuations (5). However, in contrast to the usual parcel theory, Eqs. (3) and (5) do allow the fluid element model to predict classical shear instability in the linear case (section 3) and predict fluxes and the eddy Prandtl number which depend on the Richardson number in qualitative agreement with the limited observational evidence (section 6).

e. Total equations

The above scaling arguments are indeed tentative but can be shown to be energetically consistent with prevailing interpretation of the turbulence energy budget. This is easily seen by beginning with the equations of motion of the fluid element. Using (2)–(5), neglecting reduction of buoyancy by pressure effects so that $A = 0$ and neglecting any virtual mass effect so that $\gamma^* = 1$, the basic Eqs. (1) become

$$\begin{matrix} & 1 & & 2 & & 3 & & 4 \\ dw/dt = & g\theta/\Theta & - & CuU_z & - & (u_e/L)w & - & (C_p/L)Vw \end{matrix} \tag{6a}$$

$$du/dt = \qquad -wU_z - (u_e/L)u - (C_p/L)Vu \tag{6b}$$

$$d\theta/dt = -wS \qquad - (u_e/L)\theta \tag{6c}$$

where, again, all variables are deviations of the element values from the ambient value. Equation 6 can be partitioned into several different physical mechanisms which lead to coupling between w, u and θ. The buoyancy mode (column 1) involves the buoyancy generation or destruction of vertical motion and production of buoyancy by the vertical motion acting upon the mean stratification. The shear mode (column 2) involves generation of horizontal momentum by vertical advection acting upon the mean shear and simultaneous production of vertical motion through the shear-induced pressure term (last term, Eq. 6a). The generation of element buoyancy and momentum is counteracted by linear diffusion of element properties by the smaller-scale turbulence (column 3) and nonlinear pressure drag (column 4). The representation of pressure corresponds to terms 2 and 4.

f. Comparison with previous models

If we neglect the pressure-shear generation of vertical velocity ($C = 0$), and exclude consideration of the horizontal velocity, the system (6) becomes analogous to penetrative convection model of Mahrt (1979). If we also neglect pressure drag ($C_p = 0$), the system (6) becomes analogous to the one-dimensional models of Priestley (1953, 1959). If we eliminate the pressure-shear term and small-scale diffusion terms ($C = u_e = 0$) but retain nonzero C_p, (6) becomes *mathematically* equivalent to the models of parcel motion with self-similar quadratic drag (Priestley and Ball 1955; Mason and Emig 1961, Eq. 5; Simpson and Wiggert 1969).

If we neglect the pressure-shear term, the small-scale diffusion and pressure drag, then system (6) reduces to a simple buoyancy oscillation, which, in the absence of initial parcel buoyancy, yields the vertical length scale $w(0)/N$ where $w(0)$ is the initial parcel vertical velocity and N is buoyancy frequency $(gS/\Theta)^{1/2}$.

g. Kinetic energy budget

Using (6), the equation for the kinetic energy of the element for the vertical component and the horizontal component in the mean shear direction are, respectively,

$$(1/2)\partial(w^2)/\partial t = (g/\Theta)w\theta - u_e w^2/L - (C_p/L)Vw^2 - CwuU_z \quad (7a)$$

$$(1/2)\partial(u^2)/\partial t = -uwU_z - u_e u^2/L - (C_p/L)Vu^2. \quad (7b)$$

The energy equations are most familiar when summed over many fluid elements. In (7), vertical kinetic energy is generated or suppressed by the buoyancy flux while horizontal kinetic energy is generated by the usual mean shear term proportional to the Reynold's stress. The loss of kinetic energy due to terms containing u_e corresponds to transfer of kinetic energy to smaller scales where it is eventually dissipated by viscosity. A formal analogy to dissipation can be made by equating the three-dimensional analogy of these terms to the usual formulation of dissipation of kinetic energy, in which case we obtain

$$u_e(u^2 + v^2 + w^2)/L \approx C_\epsilon(u^2 + v^2 + w^2)^{3/2}/L$$

where C_ϵ is a nondimensional coefficient thought to be $O(1)$. This suggests that u_e be of the form

$$u_e = \text{const}(u^2 + v^2 + w^2)^{1/2}$$

which would correspond to the three-dimensional analogy to the self-similar formulation of diffusion (2b). Note that the dissipation terms in (6) involving the small-scale diffusion velocity u_e are completely different from the turbulent transport of kinetic energy by itself which is often parameterized as a diffusion term. The latter effect corresponds to spatial redistribution of turbulence energy and not transfer to smaller scales. Such transport terms do not explicitly occur in (6) because the total derivative on the left-hand side is defined with respect to a moving fluid element.

Noting that wuU_z is the shear generation of the total turbulence kinetic energy, the coefficient C can be viewed as the fraction of the rate of shear generation of horizontal kinetic energy which, in turn, is converted to vertical kinetic energy via pressure effects. This conversion and associated loss of horizontal kinetic energy in the present model would be identified with the pressure drag term in the horizontal kinetic energy equation as can be visualized with the lower part of Fig. 1.

For neutrally stratified turbulent flow, the two velocity components perpendicular to the shear each typically contain about ¼ of the total turbulence kinetic energy with the remaining half of the variance occurring in the component parallel to the shear vector (Tennekes and Lumley 1972, and others); i.e., the ratio $[w^2]/[u^2]$ maintains an approximate value of 0.5 where the brackets indicate some sort of averaging. The present model (6) with equilibrium conditions and vanishing stratification, allows an analytical solution which predicts that the above velocity ratio is equal to C (section 4, Eqs. 14–15). Then, the above observations tentatively suggest that $C = 0.5$ for neutral stratification.

In the linear version of (6) where the pressure drag is neglected but the stratification is nonzero, C becomes approximately equal to the critical gradient Richardson number (section 3). Then with the approximate choice of $C = 0.25$, the linear system predicts the classical critical value and provides some support for formulation of the shear-pressure term (5).

In passing, we note that in Hinze (1975, Chapter 4), the conversion of turbulent kinetic energy from the shear-generated component to the other components is related to the difference between the kinetic energies (here $u^2 - w^2$). However, closure of this argument would require additional formulation of a time scale. We will evaluate the performance of the present model (6) in terms of prediction of fluxes in section (6).

3. Vanishing pressure drag

Some of the different flow regimes and dependence on the nondimensional parameters can be identified in terms of analytical solution by omitting the nonlinear pressure drag term from (6) in which case we obtain

$$dw/dt = g\theta/\Theta - (u_e/L)w - CuU_z \quad (8a)$$

$$du/dt = -wU_z - (u_e/L)u \quad (8b)$$

$$d\theta/dt = -wS - (u_e/L)\theta. \quad (8c)$$

As the shear vanishes, (Eq. 8) describes a linear, damped buoyancy oscillation. As the diffusion velocity vanishes, (8) describes a shear-driven buoyancy oscillation.

Equations (8a)–(8c) are linear in that they can be written in the form

$$d\phi/dt = \mathbf{F}(\phi)$$
$$\phi = [w, u, \theta] \quad (8d)$$

where $\mathbf{F}$ is a constant matrix independent of the vector of unknowns ϕ. The linear solution for ϕ is of the general form

$$A_i \exp(\lambda_i t) \quad (9)$$

where λ_i ($i = 1, 3$) are the eigenvalues for the three solution modes, and A_i are the amplitudes of the three

modes which are dependent on initial conditions. The complete linear solution which satisfies initial conditions is easily obtained but not needed here. Our interest is confined to the stability criteria for the linear equations to insure that the linear version of the present model is consistent with classical theory of shear instability.

The cubic characteristic equation for the eigenvalues is homogeneous and reduces to an easily solved quadratic equation with two independent roots. Two eigenvalues yield exponential decay while the remaining eigenvalue is of the form

$$\lambda = -(u_e/L) + U_z(C - \mathrm{Ri})^{1/2} \qquad (10)$$

where the gradient Richardson number (Ri) is defined as

$$\mathrm{Ri} \equiv (gS/\Theta)/(U_z^2).$$

For vanishing diffusion velocity, the critical Richardson number separating exponential growth from exponential decay is simply C. Classical linear stability analysis indicates a critical gradient Richardson number of 0.25 which would correspond to $C = 0.25$ in relationship (10).

For nonzero diffusion velocity, three regimes can be identified based on the Richardson number. In the very stable case ($\mathrm{Ri} > C$), the eigenvalue is complex with negative real part (damping) and nonzero imaginary part (oscillation) corresponding to damped harmonic oscillation. More specifically, the motion is a buoyancy oscillation modified by shear and damped by small-scale mixing. This flow behavior is plotted in the usual phase space in Fig. 3. With vanishing diffusion velocity u_e and vanishing mean shear, the motion for this regime becomes a pure buoyancy oscillation with frequency $(gS/\Theta)^{1/2}$.

Simple damping without oscillation (Fig. 3) corresponding to real negative eigenvalues (10) occurs for a narrow range of Richardson numbers

$$C - (u_e/U_zL)^2 < \mathrm{Ri} < C. \qquad (12)$$

Therefore the coefficient C becomes the value of the Richardson number separating two stable regimes. Instability (Fig. 3) corresponding to a real positive eigenvalue occurs when the Richardson number becomes less than the following critical value:

$$\mathrm{Ri} < C - (u_e/U_zL)^2 \equiv \mathrm{Rc}. \qquad (13)$$

That is, the small scale diffusion velocity u_e reduces the critical Richardson number for instability (right-hand side of 13) to values slightly less than C. Stronger shear is needed for instability with small-scale diffusion. However, the influence of u_e in (13) for expected geophysical values is small so that the critical Richardson number for instability defined by (13) is approximately C. In other terms, the range of Richardson numbers for simple decay (12) is small.

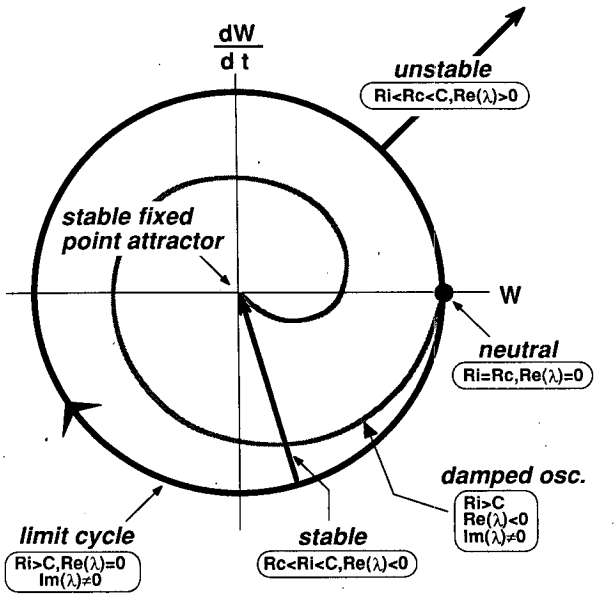

FIG. 3. Flow trajectories for different stability regimes for the linear case (8a)–(8c). Here $\mathrm{Im}(\lambda) = 0$ unless otherwise specified, and Rc is the critical Richardson number defined by (13).

The influence of the coefficient C can be examined further by combining equations (6a)–(6c) into the simple form

$$dH/dt = -2(u_e/L)H$$

$$H = w^2 - Cu^2 + (g/S\Theta)\theta^2.$$

For vanishing diffusion velocity, H is conserved. Here H is not a Hamiltonian since the shear-generation term wU_z is not a conservative "force". With nonzero diffusion, H damps to zero. This does not correspond to vanishing flow or even finite flow since H is proportional to the difference between the vertical and horizontal velocities. In fact, in the linearly unstable case both velocity components approach infinity as H vanishes.

It is of more interest that the ratio of the vertical velocity component to the horizontal velocity component is governed by the coefficient C. In the case of equilibrium flow where H vanishes, the ratio w^2/u^2 approaches C with vanishing stratification; i.e., with larger values of C, pressure effects generate vertical motions more efficiently. We will return to the dependence on C in section 4 where nonlinear pressure drag is restored and the unrealistic possibility of exponential growth is eliminated.

4. Fixed points

With the complete equations (6a)–(6c), any initial instability is soon controlled by nonlinear pressure drag as the relative motion of the fluid element becomes significant. Such control may lead to limit cycle motion

about a fixed point or evolution to a fixed point attractor depending on the mean shear and stratification and values of model coefficients. The fixed point solutions correspond to equilibrium conditions where the Lagrangian time derivative $d\phi/dt$ vanishes. Constant vertical velocity implies infinite vertical length scale. That is, height-independent stratification and mean shear may possess no natural vertical length scale as is most obvious in the case of neutral stratification. In actual geophysical flows, near-neutral layers occur over finite depths embedded within stronger stratification which provide a limiting vertical length scale for the motion. However, the fixed point solutions exert important influences on the more realistic height-dependent solutions and therefore warrant examination.

a. *Vanishing stratification*

The fixed point solution for the complete system (6a)–(6c) is mathematically obtainable but far too complex to extract obvious physical interpretation. For the case of vanishing stratification representing a balance between shear effects, small-scale diffusion and pressure drag, the fixed point solution for (6a)–(6c) simplifies to

$$u = (+/-)[C^{1/2}U_z - u_e/L]/[(C_p/L)(1 + C)^{1/2}] \tag{14}$$

$$w = -C^{1/2}u. \tag{15}$$

As expected, the magnitude of the equilibrium vertical velocity is proportional to the shear and inversely proportional to the pressure-drag coefficient. The ratio w^2/u^2 is equal to C in agreement with the linear case (section 3) in the limit of vanishing stratification. With vanishing pressure drag ($C_p = 0$), the fixed point solution approaches infinity in agreement with the unstable linear solution occurring with vanishing stratification (section 3).

For the limit of vanishing pressure-drag ($C_p = 0$), but nonzero stratification, the fixed point solution represents the following balance:

$$gS/\Theta + (u_e/L)^2 = CU_z^2 \tag{16}$$

which, in turn, implies that the Richardson number is exactly equal to the critical value defined by (13); i.e., with vanishing nonlinear drag, stationary solutions are possible only when the neutral linear stability requirement is exactly satisfied corresponding to vanishing eigenvalues and no growth or decay. Then the fixed point solution is simply the initial conditions. With infinitesimal change of the Richardson number in this case, the solutions diverge from the equilibrium point so that (16) represents a bifurcation point corresponding to structural instability.

b. *Stability of fixed points*

The fixed point solutions are most relevant to the total dynamics only if they act in some sense as attractors for the solution trajectories. In this subsection we study the stability of the flow with respect to the fixed points by expanding the nonlinear operator, corresponding to the right-hand side of (6), about the fixed point solutions of the nonlinear system (6a)–(6c) analogous to traditional analyses of the stability of fixed points (e.g., Hirsch and Smale 1974; Bergé et al. 1984; Thompson and Stewart 1986).

We write (6a)–(6c) in the form

$$d\phi/dt = F(\phi) \qquad \phi = [w, u, \theta] \tag{17}$$

and consider a perturbation solution trajectory

$$\delta\phi(t) = \phi(t) - \phi^*$$

where ϕ^* is a fixed point solution. Expanding the functional matrix $F(\phi)$ in a Taylor series about the fixed point solution, we obtain

$$d\phi/dt = F(\phi) = F(\phi^*) + DF(\phi^*)[\delta\phi] + O(\delta\phi^2) \tag{18}$$

where $DF(\phi^*)$ is the first variation of the functional matrix F with respect to the dependent variable ϕ evaluated at the equilibrium fixed point and of the form

$$DF(\phi) = \begin{cases} [-u_e/L - (C_p/L)w^*] & -CU_z & g/\Theta \\ -U_z & [-u_e/L - (C_p/L)u^*] & 0 \\ -S & 0 & -u_e/L \end{cases} \tag{19}$$

where w^* and u^* are defined as

$$w^* \equiv V(1 + w^2/V^2)$$
$$u^* \equiv V(1 + u^2/V^2)$$
$$V \equiv (u^2 + w^2)^{1/2}$$

where u and w in these relationships are evaluated at the equilibrium fixed point. Noting that

$$d(\phi^*)/dt = F(\phi^*) = 0, \tag{20}$$

(18) becomes approximately

$$d(\delta\phi)/dt = D[F(\phi^*)][\delta\phi]. \tag{21}$$

This system is linearized in that $DF(\phi^*)$ is a function only of the known vector ϕ^* and independent of $\phi(t)$. The linearization of (21) has reduced the stability problem to finding the eigenvalues of the first variation

$DF(\phi^*)$ which satisfy the following cubic characteristic equation:

$$\lambda^{*3} + \lambda^{*2}(C_p/L)(w^* + u^*) + \lambda^*[(C_p/L)^2 u^* w^* - C(U_z)^2 + gS/\Theta] + 2(gS/\Theta)(C_p/L)u^* = 0 \quad (22)$$

$$\lambda^* = \lambda + u_e/L \quad (23)$$

The coefficient of the λ^* term with zero pressure drag vanishes when the gradient Richardson number equals the critical value of C. Only in the case of vanishing pressure drag, does the above eigenvalue relationship for stability of the fixed point reduce to the traditional stability requirements of the linear system (section 3) where the solution is stable when the Richardson number exceeds a critical value of C.

Since the case of large Richardson number is controlled by damping to the motionless fixed point attractor, we wish to study the other limiting case where buoyancy effects vanish and the flow trajectories might be controlled by the fixed points (14)–(15). For vanishing buoyancy, the cubic equation for the eigenvalue (22) reduces to the following quadratic form:

$$\lambda^{*2} + \lambda^*(C_p/L)[w^* + u^*] + (C_p/L)^2 w^* u^* - C(U_z)^2 = 0 \quad (24)$$

in which case,

$$\lambda^* = -(1/2)(C_p/L)(u^* + w^*)\{1(+/-)[1 + 4(CU_z^2 - (C_p/L)^2 u^* w^*)/((C_p/L)^2(u^* + w^*)^2)]^{(1/2)}\}. \quad (25)$$

For instability to occur ($\lambda > 0$), the argument of the square root must be greater than 1 in which case the negative root leads to a positive eigenvalue. The argument of the square root is greater than 1 if

$$4CU_z^2 > (C_p/L)^2 u^* w^*. \quad (26)$$

Substituting the equilibrium solutions (14–15) into u^* and w^* (23) and then substituting into (26), we see that the right-hand side is categorically larger than the left-hand side so that the nonzero fixed point solution (14)–(15) is stable with respect to perturbations regardless of the values of the shear and coefficients C, C_p, and u_e. The fact that the eigenvalues are negative and not close to zero allow the fixed point to be stable with respect to perturbations of finite size. In fact, in the next section, we will see that the fixed points corresponding to (14)–(15) act as attractors to limit cycle solutions for a wide range of values of the Richardson number and model coefficients.

5. Limit cycle solutions

For a wide range of conditions, the solutions to (6a)–(6c) correspond to limit cycle motions influenced by two attractors defined by the equilibrium states (14–15) in addition to the motionless fixed point attractor for the simple buoyancy oscillation. The limit cycle motions can be viewed as idealized elements participating in shear-driven overturning as would occur with transverse vortices. This conceptual possibility is appropriate only in a statistical sense since actual individual eddies have finite lifetimes.

To obtain solutions of the nonlinear system, (6a)–(6c) was solved using a fourth-order Runge–Kutta scheme. Initial conditions are zero temperature perturbation, no initial horizontal flow, and an initial vertical velocity of 0.001 m s^{-1}. For the parameter regions examined and *small* initial values of the element motion and buoyancy, the final state for w, u and θ is insensitive to the exact values of the initial conditions.

Numerical evaluation of (6a)–(6c) for expected geophysical values of the diffusion velocity (lower part of Figure 4), limit cycle motion is established for an intermediate range of Richardson numbers with near-motionless fixed point solutions at large Richardson number and nonzero fixed point motion at small Richardson numbers. The amplitude of the near-motionless fixed point is negligible from a geophysical point of view and decreases with further increases of the Richardson number. Large values of the diffusion velocity shrink the range of Richardson numbers which permit limit cycle motion (Fig. 4) and the limit cycle motion vanishes altogether for very large values of the diffusion velocity. That is, large diffusion velocity acts to damp the time-dependent deviation from fixed point solutions.

From another point of view, the value of the critical Richardson number separating near-motionless flow from the limit cycle motion increases with decreasing diffusion velocity (Fig. 4) and the critical Richardson number becomes infinity with vanishing diffusion velocity. In the latter case, the limit cycle motion becomes a simply buoyancy oscillation at large Richardson numbers. This critical Richardson number is physically

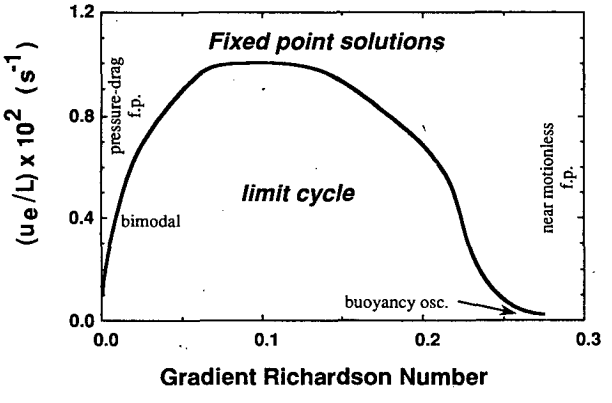

FIG. 4. The main eddy regimes as a function of diffusion velocity and gradient Richardson number for $C_p/L = 0.005$. These regimes are insensitive to the value of C_p/L for the expected geophysical range of parameter values. The lower part of the graph is most relevant to geophysical flows.

different from that for the linear case since unlimited exponential growth is now removed by the nonlinear pressure drag and the flow at Richardson numbers higher than the critical value does not completely vanish. Therefore, the critical Richardson number for the nonlinear case represents a transition between two nonzero finite flows instead of a transition between exponential growth and exponential decay. In the nonlinear case, the dependence on the Richardson number is no longer unique even with fixed values of the other coefficients. For example, with stronger stratification, the critical Richardson number is somewhat larger; i.e., the nonlinear flow depends on the magnitude of the shear and stratification in addition to their ratio, although the occurrence of the basic flow regimes depend mainly on the Richardson number and diffusion velocity.

Although the general location of the above flow regimes in the diffusion velocity–Richardson number phase space (Figure 4) does not depend significantly on the value of the pressure drag coefficient, the amplitude of the both the limit cycle motion and the fixed point flow decrease with increasing pressure drag coefficient as predicted by (14)–(15). As the pressure drag coefficient becomes hypothetically large, the amplitude of the limit cycle motion eventually becomes geophysically negligible and thus indistinguishable from near-motionless fixed point conditions.

The amplitude of the vertical motion, W_{amp}, and the vertical depth of the limit cycle motion ℓ are related as

$$\ell = C_\ell W_{amp}/N$$

where N is the buoyancy frequency and C_ℓ is a coefficient whose value is between 3 and 4 for the range of parameter values examined. This coefficient becomes about one-third smaller if the amplitude of the vertical motion is replaced by the root mean square of the vertical velocity. For cases of height-dependent Richardson number, the depth of the layer of small Richardson numbers permitting motion development becomes the main vertical constraint if it is smaller than the depth ℓ. The period of the limit cycle motion is longer than the buoyancy period due to the increase of the depth of the motion associated with the mean shear.

As the Richardson number decreases, the limit cycle motion becomes more influenced by the two nonzero fixed points representing a balance between shear-generation, pressure-drag, and diffusion (14)–(15). The influence of these fixed points distorts the limit cycle motion (Fig. 5) from the sinusoidal buoyancy oscillation occurring at large Richardson numbers. With sufficiently strong shear and weak buoyancy, the two lobes of the limit cycle break apart and the solution collapses to one of the two fixed points. The transition from the bimodal limit cycle to the nonzero fixed point flow defines a second transitional Richardson number whose value increases with increasing diffusion velocity.

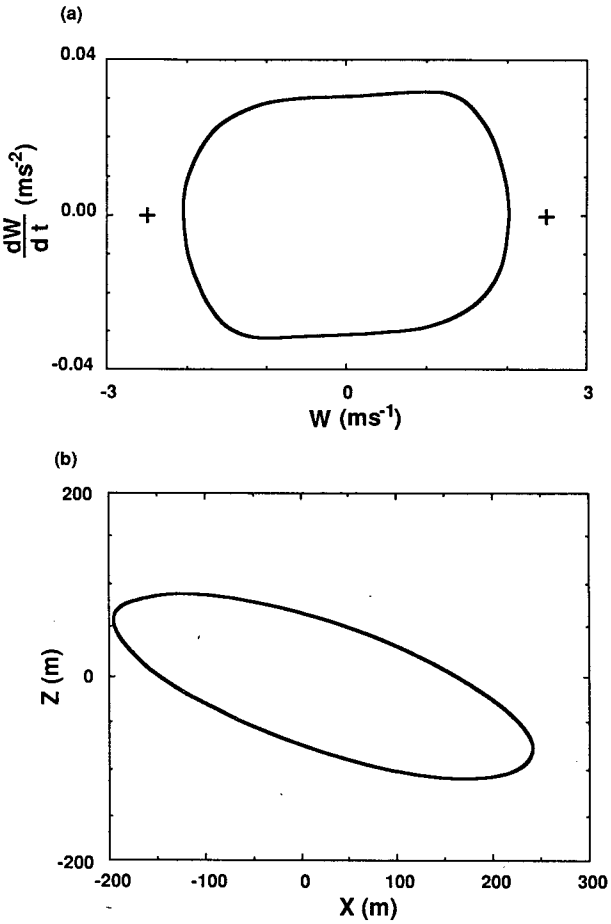

FIG. 5. Bimodal limit cycle in (a) $w - w_l$ phase space and (b) x–z space for $u_e/L = 0.002$ and $C_p/L = 0.005$ for height-independent mean shear [6 m s^{-1} (100 m^{-1})] and stratification [2 K (100 m)]. The fixed point solutions from Eqs. (14)–(15) (plus symbols) overpredict the motion strength because of neglect of stratification. With weaker stability, the limit cycle motion becomes more bimodal in phase space and becomes less flat in x–z space.

These nonzero fixed point solutions in pure form are only of academic interest since in geophysical flows additional length scales are imposed by the height dependence of the Richardson number. With more realistic vertical structure, the vertical thickness of layers of small Richardson number constrains the vertical development of the motion. This leads to limit cycle motion even when the Richardson number is locally smaller than the transitional value for the case of height-independent shear and stratification. The behavior of the limit cycle motion for the more general case becomes difficult to summarize further since the vertical mean profiles may assume an infinite variety of forms. When the direction of the mean shear varies with height, an additional equation analogous to (6b) is needed for the other horizontal component of momentum. In spite of these complications, the shear-drag fixed point solutions predicted by height-inde-

pendent shear remain an important influence on the more complicated limit cycle motion.

The aspect ratio of the limit cycle motion is sensitive to the choice of the parameter C which controls the rate at which horizontal kinetic energy is converted to vertical kinetic energy through implied pressure fluctuations (section 2c). The influence of the value of C on the aspect ratio of the limit cycle eddies can be concisely predicted by multiplying (6a) by w and (6b) by u, integrating over one limit cycle, using the fact that the variables return to their same values after one limit cycle, and finally noting that integrated time derivatives vanish. We then obtain for the velocity components:

$$P(w^2) = (g/\Theta)[w\theta] - C[uw]U_z P(u^2) = -[uw]U_z \tag{27}$$

where square brackets indicate integration over one limit cycle and the operator P defines integration over one limit cycle in the following form:

$$P \equiv \left\{(u_e/L)\int + (C_p/L)\int V\right\}. \tag{28}$$

Then, we obtain

$$P(w^2)/P(u^2) = (C - \mathrm{Rf}) \tag{29}$$

where the flux Richardson number is defined as

$$\mathrm{Rf} \equiv (g/\Theta)[w\theta]/[wu]U_z. \tag{30}$$

As the *flux* Richardson number approaches the value of C, the vertical motions vanish even in the linear case of vanishing C_p. The vertical kinetic energy is larger for larger values of C since this coefficient represents the efficiency at which vertical motions are generated from shear-induced pressure fluctuations.

6. Eddy transport

With vanishing diffusion velocity, the heat flux averaged over one limit cycle also vanishes. In this case, the limit cycle motion is just recirculating the same fluid. However, distortion of the limit cycle motion by pressure effects leads to net momentum flux even with vanishing diffusion velocity.

With nonzero small scale diffusion, limit cycle motions lead to net heat transport since mixing occurs between the element and the ambient fluid at all levels and the element is no longer recirculating the same fluid. For example, in a stratified ambient flow, the downdrafts of the elements will be warmer than the updrafts. In still other terms, the small-scale diffusion alters the phase between vertical motion and other variables leading to net vertical transport even when averaged over one limit cycle.

The vertical fluxes and eddy diffusivities predicted by the modeled Lagrangian element are of considerable practical interest. With the present approach, a priori constraints are not imposed on the eddy diffusivity or the length scale of the vertical mixing. Instead, the pressure drag coefficient and diffusion velocity must be specified. We therefore need to evaluate the behavior of the eddy diffusivities predicted by the limit cycle model as they relate to the Richardson number, diffusion velocity and pressure drag coefficient. To study the dependence on the Richardson number, we choose plausible values of $u_e/L = 0.002$ and $C_p/L = 0.005$.

The eddy diffusivities computed from the limit cycle motions exhibit the expected decrease with increasing Richardson number (Fig. 6) and drop to negligible values as the Richardson number exceeds the critical value. At small Richardson numbers, the diffusivity for heat may become comparable to or larger than the eddy diffusivity for momentum (Prandtl number O(1)) depending mainly on the value of the diffusion velocity. At larger Richardson numbers, the diffusivity for momentum exceeds that for heat (Prandtl number > 1) due to momentum transport by pressure fluctuations associated with nonzero C_p.

At very small Richardson numbers, the vertical length scale of the limit cycle motion and the eddy exchange coefficients become unrealistically large in the present artificial case of height-independent shear and stratification. With more realistic profiles of shear and stratification, the layers of small Richardson number are of limited thickness which constrains the depth of the modeled limit cycle motions (section 5) which, in turn, reduces the eddy diffusivities resulting from the limit cycle motions. The "best" values for these coefficients probably also depend on the grid defining the mean profiles, whether from data or from a larger-scale model. For example, with crude vertical resolution, the Richardson number for the layer between grid levels may be large while, in reality, turbulence still occurs but on smaller scales. This possibility suggests use of a smaller value of u_e than in the present study.

The dependence of the flux and diffusivities on the values of the pressure-drag coefficient and the diffusion velocity can be seen by multiplying (6b) by u and (6c) by θ and integrating over one limit cycle. Again, using the fact that a given variable returns to the same value after one limit cycle, we obtain

$$[wu] = -(1/LU_z)\{u_e[u^2] + C_p[u^2V]\} \tag{31}$$

$$[w\theta] = -(u_e/LS)[\theta^2] \tag{32}$$

where the brackets [ ] indicate averaging over one limit cycle. The fluxes not only vanish as C_p and u_e vanish (simple buoyancy oscillation), as explicitly revealed by (31)–(32), but also vanish as C_p and u_e approach very large values where the motion is completely damped, and dependent variables on the right-hand side of (31)–(32) vanish. Numerical solution of (6a)–(6c) for expected geophysical ranges of the diffusion velocity and pressure drag coefficient, indicates that the magnitude of the eddy diffusivities depend inversely

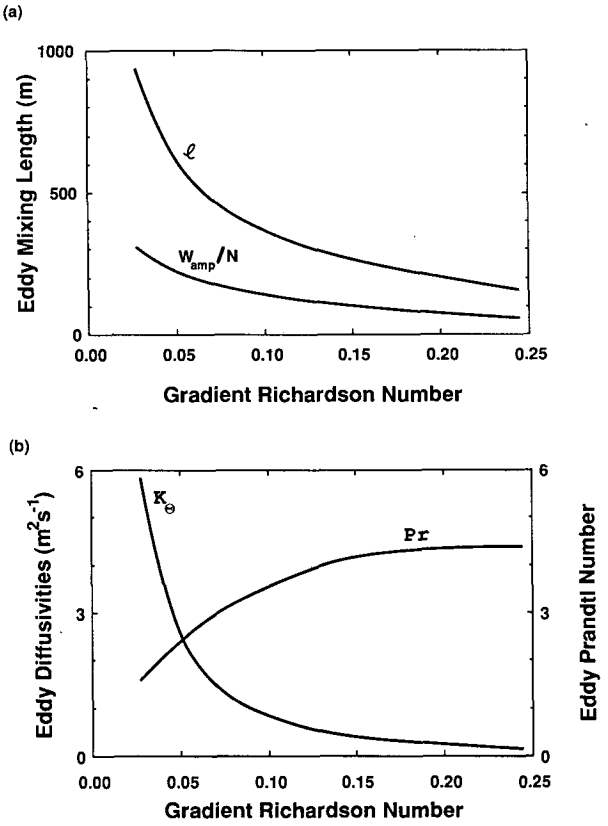

FIG. 6. (a) The vertical depth of the motion ℓ for the limit cycle eddies and parcel depth scale $w_{amp}\,N^{-1}$ and (b) the eddy diffusivity for heat (K_θ) and Prandtl number (Pr) as a function of Richardson number for $C_p/L = 0.005.$, $u_e/L = 0.002$ and $C = 0.25$. The critical Richardson number for this case occurs at approximately 0.24 above which the limit cycle motion collapses to near zero fixed point motion. The critical Richardson number increases with increasing C and decreasing u_e.

on the pressure drag coefficient through reduction of motion amplitude while the dependence on the diffusion velocity depends on situation.

Relationships (31)–(32) verify that only the heat flux vanishes with vanishing diffusion velocity while the momentum flux remains nonzero with nonzero pressure drag C_p. More specifically, the eddy Prandtl number

$$\mathrm{Pr} = K_u/K_\theta = \{[wu]/U_z\}/\{[w\theta]/S\}$$

corresponding to (31)–(32) is of the form

$$\mathrm{Pr} = \{S^2/U_z^2\}\{(C_p/u_e)[Vu^2] + [u^2]\}/[\theta^2]. \quad (33)$$

The dependence of the eddy Prandtl number on the ratio (C_p/u_e) reflects the transport of momentum by the modeled pressure term. However, the amplitude of the limit cycle motion is inversely related to the pressure drag coefficient in such a manner that the net influence of the pressure drag coefficient on the Prandtl number (33) is small. The Prandtl number decreases with increasing diffusion velocity corresponding to the relative increase of heat transport; i.e., with large diffusion velocity, the transport by pressure effects is no longer as important.

Relationship (33) also indicates the expected increase of the Prandtl number with increasing Richardson number as can be seen from the first factor on the right-hand side. With large Richardson number, the flow becomes more like a shear-modified buoyancy oscillation which transports momentum through pressure effects but does not efficiently transport heat. Numerical evaluation of (6a)–(6c) indicates that the increase of the Prandtl number with Richardson number tapers off as the Richardson number approaches the critical value (Fig. 6).

The model can therefore be "tuned" by adjusting the pressure drag to produce the expected magnitude of the eddy diffusivity for heat, and adjust the value of the diffusion velocity to produce the expected magnitude of the Prandtl number. This adjustment must recognize that the critical Richardson number increases with decreasing u_e and increases with increasing C.

While the measurement of eddy diffusivities from geophysical and laboratory data are vulnerable to various measurement and sampling problems, we briefly compare the eddy Prandtl number predicted by the limit cycle model with that inferred from data. The eddy Prandtl number in the atmosphere appears to be as large as O(10) in very stable conditions (Kondo et al. 1978; Mahrt 1985) and on the order of 2 or 3 above the surface layer with modest stability (Lenschow et al. 1988, their Fig. 12). Laboratory studies also indicate an increase of the Prandtl number with increasing Richardson number (Webster 1964; Arya 1975; Mizushina et al. 1978; Rohr et al. 1988) although the above studies disagree on the magnitude of the Prandtl number. The decrease of the Prandtl number with increasing gradient Richardson number is presumably due to the transport of momentum by pressure fluctuations possibly associated with internal gravity waves.

The above results are based on constant diffusion velocity. One might iteratively relate the magnitude of the diffusion velocity to the velocity of the element motion averaged over one limit cycle and adjust L to be proportional to the depth scale of the limit cycle motion. However, this possible improvement is too complex for present goals.

7. Conclusions

The Lagrangian equations for idealized turbulent motions (6a)–(6c) determine the fluxes in terms of gradients on the scale of the transporting eddies. As with the approaches of Stull (1984) and Fiedler (1984), the present approach avoids problems encountered with the usual gridded models where modeled fluxes are related to the gradients computed between adjacent grid levels regardless of the scale of the transporting

eddies. The present approach also avoids specification of mixing lengths or eddy diffusivities but does require specification of several other coefficients and is more complicated than mixing length theory even with the restrictions imposed in this study.

A key formulation in the present limit cycle mixing model is the generation of vertical motions by pressure fluctuations induced by shear-driven horizontal velocity fluctuations. This formulation leads to consistency with the usual simple energy arguments and, in the linear case, predicts the usual critical gradient Richardson number. In the nonlinear case, the critical Richardson number may be considerably larger depending on the value of the small-scale diffusion velocity and represents the transition between limit cycle motions (steady periodic) and very weak flow.

For large Richardson number, the limit cycle is controlled by the fixed point solution corresponding to motionless flow. As the Richardson number decreases, the element motion becomes distorted by the attraction of two additional fixed points associated with shear and drag.

The amplitude of the motion and values of the diffusivities decrease with increasing pressure drag coefficient. The eddy diffusivities predicted by the limit cycle motion decrease smoothly with increasing Richardson number and then decrease sharply at the critical Richardson number. The eddy Prandtl number increases with Richardson number since the transport of momentum by pressure effects remains important while the heat and mass transport is reduced by the stability.

Obvious improvements to the model include extension to three dimensions, generalization of the mixing-entrainment formulation allowing for changing size and diffusion velocity of the fluid element, adoption of a more complete formulation of the pressure terms and application to shallow moist convection. However, these improvements would compromise the physical and mathematical simplicity of the present model. The details of application of the limit cycle equations to formulate mixing in larger scale models, including the "best" choice of values of the coefficients, will probably depend on the specifics of the larger-scale model including vertical resolution. The model might also be applied to dispersion problems where equations (6a)–(6c) map an initial distribution of parcels into a new distribution at a later time. In this case, random forcing as in Csanady (1964) and Pearson et al. (1983) might be appropriate.

Acknowledgments. The useful comments of Mark Hadfield, Roland Stull, Jin-Won Kim, Nimal Gamage, Carl Hagleberg, Kenneth Mitchell, and John Dutton are greatly appreciated as is the computational work of Gayani Gamage. This material is based upon work supported by Air Force Geophysics Laboratory under Contract F 19628-88-K-0001 and the Meteorology Program of the National Science Foundation under Grant ATM-8521349. Part of this work was carried out while a visitor to the Geophysics Institute, University of Bergen, and the Bergen Scientific Centre.

REFERENCES

Arya, S. P. S., 1975: Buoyancy effects in a horizontal flat-plate boundary layer. *J. Fluid Mech.*, **68,** 321–343.

Batchelor, G. K., 1951: Pressure fluctuations in isotropic turbulence. *Proc. Cambridge Phil. Soc.*, **47,** 359–374.

Bergé, P., Y. Pomeau and C. Vidal, 1984: *Order Within Chaos.* Wiley & Sons, 329 pp.

Csanady, G. T., 1964: Turbulent diffusion in a stratified fluid. *J. Atmos. Sci.*, **21,** 439–447.

Deardorff, J. W., 1966: The counter gradient heat flux in the lower atmosphere and in the laboratory. *J. Atmos. Sci.*, **23,** 503–506.

Dutton, J. A., and G. H. Fichtl, 1969: Approximate equations of motion for gases and liquids. *J. Atmos. Sci.*, **26,** 241–254.

Fiedler, B. H., 1984: An integral closure model for the vertical turbulent flux of a scalar in a mixed layer. *J. Atmos. Sci.*, **41,** 674–680.

Hinze, J. O., 1975: *McGraw Hill Series in Mechanical Engineering.* McGraw Hill, 790 pp.

Hirsch, M. W., and S. Smale, 1974: *Differential Equations, Dynamical Systems, and Linear Algebra.* Academic Press, 358 pp.

Kondo, J., O. Kanechika and N. Yasuda, 1978: Heat and momentum transfer under strong stability in the atmospheric surface layer. *J. Atmos. Sci.*, **35,** 1012–1021.

Krasnoff, E., and R. L. Peskin, 1971: The Langevin model for turbulent diffusion. *Geophys. Fluid Dyn.*, **2,** 123–146.

Lenschow, D., Xing Sheng Li, Cui Juan Zhu and B. Stankov, 1988: The stably stratified boundary layer over the Great Plains. *Bound.-Layer Meteor.*, **42,** 95–121.

Levine, J., 1959: Spherical vortex theory of bubble-like motion in cumulus clouds. *J. Meteor.*, **16,** 653–662.

Lin, C. C., and W. Reid, 1963: Turbulent flow: theoretical aspects. *Handbuch der Physik,* vol. VII/2, S. Flügge, Ed., Springer, 438–523.

List, R., and E. P. Lozowski, 1970: Pressure perturbations and buoyancy in convective clouds. *J. Atmos. Sci.*, **27,** 168–170.

Mahrt, L., 1979: Penetrative convection at the top of a growing boundary layer. *Quart. J. Roy. Meteor. Soc.*, **105,** 469–485.

——, 1985: Vertical structure and turbulence in the very stable boundary layer. *J. Atmos. Sci.*, **42,** 2333–2349.

——, 1986: On the shallow motion approximations. *J. Atmos. Sci.*, **43,** 1036–1044.

Mason, B. J., and R. Emig, 1961: Calculations of the ascent of a saturated buoyant parcel with mixing. *Quart. J. Roy. Meteor. Soc.*, **87,** 212–222.

Mizushina, T., F. Ogino, H. Ueda and S. Komori, 1978: Buoyancy effect on eddy diffusivities in thermally stratified flow in an open channel. *Heat Transfer,* **1,** 91–96.

Moeng, C. H., and J. C. Wyngaard, 1986: An analysis of closures for pressure-scalar covariances in the convective boundary layer. *J. Atmos. Sci.*, **43,** 2499–2513.

Monin, A. S., and A. M. Yaglom, 1971: *Statistical Fluid Mechanics: Mechanics of Turbulence,* Vol. 1, J. Lumley, Ed., M.I.T. Press, 769 pp.

Nayfeh, A. H., and D. T. Mook, 1979: *Nonlinear Oscillations.* Wiley & Sons.

Pearson, H. J., J. S. Puttock and J. C. R. Hunt, 1983: A statistical model of fluid-element motions and vertical diffusion in a homogeneous stratified turbulent flow. *J. Fluid Mech.*, **129,** 219–249.

Priestley, C. H. B., 1953: Buoyant motion in a turbulent environment. *Aust. J. Phys.*, **25,** 135–138.

——, 1959: *Turbulent Transfer in the Lower Atmosphere.* University of Chicago Press.

——, and F. K. Ball, 1955: Continuous convection from an isolated source of heat. *Quart. J. Roy. Meteor. Soc.*, **81**, 144–157.

Rohr, J. J., E. C. Itsweire, K. N. Helland and C. W. Van Atta, 1988: Growth and decay of turbulence in a stably stratified shear flow. *J. Fluid Mech.*, **195**, 77–111.

Simpson, J., and V. Wiggert, 1969: Models of precipitating cumulus towers. *Mon. Wea. Rev.*, **97**, 471–489.

Speziale, C. G., 1987: On nonlinear $k - l$ and $k - \epsilon$ models of turbulence. *J. Fluid Mech.*, **178**, 459–475.

Stull, R. B., 1984: Transilient turbulence theory. Part I: The concept of eddy mixing across finite distances. *J. Atmos. Sci.*, **41**, 3351–3367.

Telford, J. W., 1970: Convective plumes in a convective field. *J. Atmos. Sci.*, **27**, 347–358.

Tennekes, H., and J. L. Lumley, 1972: *A First Course in Turbulence.* M.I.T. Press, 300 pp.

Thompson, J. M. T., and H. B. Stewart, 1986: *Nonlinear Chaos and Dynamics.* Wiley and Sons, 376 pp.

Turner, J. S., 1973: *Buoyancy Effects in Fluids.* Cambridge University Press, 367 pp.

Webster, C. A. G., 1964: An experimental study of turbulence in a density-stratified shear flow. *J. Fluid Mech.*, **19**, 221–245.

Wyngaard, J. C., 1984: Toward convective boundary layer parameterization: A scalar transport module. *J. Atmos. Sci.*, **41**, 1959–1969.

——, and R. A. Brost, 1984: Top-down and bottom-up diffusion of a scalar in the convective boundary layer. *J. Atmos. Sci.*, **41**, 102–112.

Zhang, D., and R. A. Anthes, 1982: A high-resolution model of the planetary boundary layer-sensitivity tests and comparisons with SESAME-79 data. *J. Appl. Meteor.*, **21**, 1594–1607.